HHS Public Access

Author manuscript

Mayo Clin Proc. Author manuscript; available in PMC 2016 June 01.

Published in final edited form as:

Mayo Clin Proc. 2015 June ; 90(6): 773–785. doi:10.1016/j.mayocp.2015.03.022.

Motor and non-motor circuitry activation induced by subthalamic nucleus deep brain stimulation (STN DBS) in Parkinson's disease patients: Intraoperative fMRI for DBS

Emily J. Knight, PhD[1], **Paola Testini, MD**[1], **Hoon-Ki Min, PhD**[1,2], **William S. Gibson, BS**[1], **Krzysztof R. Gorny, PhD**[3], **Christopher P. Favazza, PhD**[3], **Joel P. Felmlee, PhD**[3], **Inyong Kim, BS**[1], **Kirk M. Welker, MD**[3], **Daniel A. Clayton, MD**[4], **Bryan T. Klassen, MD**[5], **Su-youne Chang, PhD**[1,2,**], and **Kendall H. Lee, MD, PhD**[1,2,**]

[1]Department of Neurologic Surgery, Mayo Clinic, Rochester, MN

[2]Department of Physiology and Biomedical Engineering, Mayo Clinic, Rochester, MN

[3]Department of Radiology, Mayo Clinic, Rochester, MN

[4]Department of Neurosurgery, Swedish Medical Center, Seattle, WA

[5]Department of Neurology, Mayo Clinic, Rochester, MN

Abstract

Objective—To test the hypothesis suggested by previous studies that subthalamic nucleus (STN) deep brain stimulation (DBS) in patients with PD would affect the activity of both motor and non-motor networks, we applied intraoperative fMRI to patients receiving DBS.

Patients and Methods—Ten patients receiving STN DBS for PD underwent intraoperative 1.5T fMRI during high frequency stimulation delivered via an external pulse generator. The study was conducted between the dates of January 1, 2013 and September 30, 2014.

Results—We observed blood oxygen level dependent (BOLD) signal changes (FDR<.001) in the motor circuitry, including primary motor, premotor, and supplementary motor cortices, thalamus, pedunculopontine nucleus (PPN), and cerebellum, as well as in the limbic circuitry, including cingulate and insular cortices. Activation of the motor network was observed also after applying a

Corresponding Author: Kendall H. Lee, M.D., Ph.D., Department of Neurologic Surgery and Department of Physiology and Biomedical Engineering, Mayo Clinic Rochester, Postal Address: 200 First Street SW, Rochester, MN 55905, lee.kendall@mayo.edu. Co-corresponding Author: Su-youne Chang, Ph.D., Department of Neurologic Surgery and Department of Physiology and Biomedical Engineering, Mayo Clinic Rochester, Postal Address: 200 First Street SW, Rochester, MN 55905, chang.suyoune@mayo.edu.

Disclosure The authors have no personal financial or institutional interest in any of the drugs, materials, or devices described in this article.

Author Contributions: Conceived and designed the experiments: EJK HKM SYC KHL. Performed the experiments: EJK HKM WSG DAC BTK SYC KHL. Analyzed the data: EJK PT HKM. Contributed reagents/materials/analysis tools: KRG CPF JPF IK KMW. Wrote the paper: EJK PT HKM SYC KHL.

ClinicalTrials.gov (I.D. # NCT01809613)

Bonferroni correction (p<.001) to our dataset, suggesting that, across subjects, BOLD changes in the motor circuitry are more consistent compared to those occurring in the non-motor network.

Conclusions—These findings support the modulatory role of STN DBS on the activity of motor and non-motor networks, and suggest complex mechanisms at the basis of the efficacy of this treatment modality. Furthermore, these results suggest that, across subjects, BOLD changes in the motor circuitry are more consistent compared to those occurring in the non-motor network. With further studies combining the use of real time intraoperative fMRI with clinical outcomes in patients treated with DBS, functional imaging techniques have the potential not only to elucidate the mechanisms of DBS functioning, but also to guide and assist in the surgical treatment of patients affected by movement and neuropsychiatric disorders.

Keywords

Deep Brain Stimulation (DBS); Functional Magnetic Resonance Imaging (fMRI); Subthalamic Nucleus; Parkinson Disease

Introduction

Deep brain stimulation (DBS) is an effective treatment option for movement disorders, including Parkinson disease (PD), essential tremor, and dystonia,[1,2] and its applications are expanding to other neurological and neuropsychiatric disorders such as epilepsy,[3] chronic pain,[4] obsessive-compulsive disorder,[5] Tourette's syndrome,[6] and major depression.[7]

The main brain targets for DBS treatment of PD are the subthalamic nucleus (STN) and the globus pallidus internus.[8] Although they share commonalities in efficacy, STN stimulation seems to be more commonly correlated with neuropsychological and behavioral alterations, even though this association is still subject to investigation.[8,9] These effects would be concordant with the studied basal ganglia connections, whereby STN has been shown to connect to motor, limbic, and associative networks.[10–13]

Although a large number of patients affected by movement disorders have been effectively treated with DBS, the exact mechanisms that lead to this success are still elusive.[13,14] Because of the similar efficacy of DBS to lesion surgeries, the first hypothesis concerning the mechanism of DBS advocated the inhibition of the targeted area and consequent facilitation of the basal ganglia direct pathway.[10] However, it is now established that DBS can function through more complex mechanisms such as antidromic and orthodromic activation of STN input and output regions, modulation of complex circuits, and normalization of STN neuronal activity.[13–17]

In order to characterize DBS mechanisms, the functional connectivity of the STN as well as the brain regions that may mediate the clinical efficacy of this treatment are still subject to investigation. The cortical activity during STN DBS has been studied with electrophysiology and cortex excitability studies in rodent, non-human primate (NHP), and human subjects,[16,18–24] and with optogenetic techniques in rodents.[25]

These studies are of fundamental importance in mapping the relationships and effects of STN activity on other areas related to motor, limbic, and associative functions, and target

each component of these networks with high specificity and selectivity. However, because of the complex role and interactions of the basal ganglia, techniques that are able to globally assess brain function and activity, such as functional magnetic resonance imaging (fMRI) and positron emission tomography (PET), must also be implemented to elucidate the effects of DBS.[26] fMRI in particular is able to evaluate global brain activation with high temporal and spatial resolution.

To date, single-case or small group studies have utilized fMRI or PET imaging to investigate brain activity in PD patients undergoing STN DBS, reporting changes in the activity of sensorimotor cortex, premotor cortex, supplementary motor area, basal ganglia, thalamus, cerebellum, prefrontal cortex, cingulate gyrus, insular cortex, and brainstem.[27–32] To investigate the neural circuitry associated with basal ganglia stimulation, we previously developed a method for fMRI in swine[33] and NHP,[34] reporting increase activation in the sensorimotor associative and limbic networks by STN DBS.

In this study, we adopted an intraoperative 1.5T fMRI design and studied the blood oxygen level dependent (BOLD) response induced by STN DBS in ten patients affected by PD. We aimed to expand upon previous studies by translating the use of intraoperative fMRI during DBS to the clinical environment. With this development we tested the hypothesis supported by previous findings that STN DBS would lead to both motor and non-motor functional neural network activation.

Materials and Methods

Safety Testing

A phantom study was performed to assess radiofrequency (RF) induced heating at the DBS lead tips using the methods described by the American Society for Testing and Materials in ASTM F2182-11a.[35] For this study, a DBS electrode (Model 3387, Medtronic Inc, Minneapolis, MN) was placed in a polyacrylic gelled saline head-and-trunk phantom, designed to mimic the tissue heat transfer properties,[35] such that the orientation of the lead and extension wiring would replicate that of the electrode in a patient (Figure 1B). The electrode was connected to a percutaneous lead extension (Medtronic Model 3550, Minneapolis, MN) and a custom extension wire which extended outside the MR scan room to allow stimulation using an external device (DualScreen 3628 Medtronic. Medtronic, Inc., Minneapolis, MN).[36] During MRI scanning, temperatures at the DBS electrodes and inside the phantom were monitored using fluoroptic temperature probes placed on each of the most distal and proximal contacts of the DBS electrode as shown in Figure 1B (.8-mm tip, STF-2, Luxtron 750 system, Lumasens, Santa Clara, CA). Identical pulse sequences used in the patient studies were tested, including the gradient echo-echo planar imaging (GE-EPI) sequence and MPRAGE. The scanner specific absorption rate (SAR) predictions for the phantom study were calculated based on an assumed patient weight of 50kg, however, in the patient study patient-specific SAR values were based on individual patient weight.

Subjects

Ten subjects scheduled for STN DBS surgery for treatment of PD were recruited. Informed consent was obtained from all subjects prior to participation. All study procedures were approved by Mayo Clinic Institutional Review Board and were performed in compliance with Health Insurance Portability and Accountability Act guidelines. The study was registered at ClinicalTrials.gov (I.D. # NCT01809613). The study was completed between January 1, 2013 and September 30, 2014.

The group of patients included 5 males and 5 females, of a mean (±standard deviation, SD) age at surgery of 61.8 (±8.6) years. Mean (±SD) duration of disease before surgery was 10.2 (±4.4) years. UPDRS-III scores (range 0–108) were recorded: preoperatively, off and on levodopa; postoperatively off levodopa; at the last follow-up, off levodopa and with the stimulation on at optimized settings (Table 1). We report the optimal contact combination and stimulation settings at the latest follow-up programming session (Table 1). One patient (Patient 7) was referred from and performed programming at another institution and therefore we cannot provide related data (UPDRS-III scores, optimal stimulation settings).

Functional Imaging

During DBS lead implantation surgery, a percutaneous lead extension was connected to the DBS electrode and tunneled through the skin, a second percutaneous lead extension was connected and extended out of skin. The head frame was removed and the patient was moved to the intraoperative MRI (intra-OR-MRI) for the fMRI studies (Figure 1A). A custom extension wire was connected to the lead extension and then to a handheld pulse generator (DualScreen 3628 Medtronic. Medtronic, Inc., Minneapolis, MN) located outside the scan room.

Studies were conducted in a 1.5 T intra-OR-MRI scanner (General Electric Healthcare, Wakasha, WI, 16x, Signa software). For all sequences, a manufacturers standard transmit/receive RF head coil was used (GE Healthcare,1.5-T Quad Head Coil, model 46-28211862). fMRI was acquired using a two-dimensional GRE-EPI: TR/TE: 3000/27, flip angle: 90, FOV: 22 cm x 22 cm, matrix: 64 x 64, slice thickness 3.0 mm with 1.5 mm gap for 5 patients and slice thickness 3.5 mm with 0 mm gap thickness for the remaining 5 patients. For each acquisition, 135 volumes (the first 5 volumes were discarded for scanner equilibrium) were acquired using a block paradigm with five 6 second stimulation periods (two volumes) alternated with six 60 second rest periods (20 volumes) for a total scan time of 6 minutes 45 seconds per scan.[34] Initial DBS effect was tested during an awake DBS surgery procedure, testing 0(−)–3(+) contact stimulation with a handheld pulse generator prior to the fMRI scan. Patients showed initial symptom improvement in the operating room using 2V amplitude, 90μs pulse width, 130–185Hz frequency. Five patients underwent the fMRI study on the day of the pulse generator implantation under general anesthesia; the other five patients on the day of lead implantation conducting awake fMRI. Following the fMRI, the second externalized percutaneous lead extension was removed.

Data Analysis and Statistics

The fMRI data were subjected to a standard pre-processing steps implemented in Brain Voyager QX software (Maastricht, the Netherlands), including slice scan time correction, 3D motion correction, temporal filtering (High-pass: Fourier basis set- 5 cycles, and low-pass: Gaussian filter-FWHM 3.1 sec), and spatial smoothing (Gaussian filter with FWHM: 2.0 pixel size). FMRI data were then co-registered to the anatomical MP-RAGE images using corresponding points-based alignment and normalized to the Talairach brain coordinate system. For right-sided stimulation data was mirrored to corresponding voxels on the left side of the brain in order to be analyzed together with left-sided stimulation data. Functional activation maps (t-maps) were generated using a double-gamma hemodynamic response function (onset 0 s, time to response peak 5 s, time to undershoot peak 15 s) representing the block design for each voxel. Group analyses were computed using a fixed effects analysis to concatenate the data from all subjects after registration of voxels in Talairach space and thus integrate the data from multiple subjects into a single general linear model (GLM) analysis (Brain masking applied to reduce the number of voxels for GLM).

To correct for multiple comparisons and exclude false positive voxels, we applied False Discovery Rate (FDR<.001). In addition to and separate from the FDR, we applied the Bonferroni correction ($p<.001$) to the original data. The brain areas that survived Bonferroni correction are listed in Table 2. While FDR are widely accepted correction method, Bonferroni correction allows for a more stringent analysis than FDR, in that it considers the number of multiple comparisons, and based on this number corrects the p-value required for each voxel to reach the desired significance level.[37]

Cortex Based Alignment

A cortex based alignment was performed, segmenting the gray/white matter boundary of the hemispheres using an automatic segmentation process based on intensity histograms. The cortices from individual subjects were then aligned through transformation into spherical representations and non-rigid alignment to the group average in an iterative coarse-to-fine process. After cortex-based alignment, group analysis as described above was repeated in this new standard surface space. To exclude false positive voxels and correct for multiple comparisons, we only considered surface voxels with a significance level FDR<.001.

Results

Phantom Testing

Prior to application in patients, heat induction at the DBS electrode contacts was measured in a head and trunk phantom during GE-EPI and 3D MP-RAGE sequences. Both sequences generated heating well below 1°C. Expectedly, the RF-heating of the DBS lead tips during the GRE-EPI fMRI sequence (SAR=.016W/kg; $\Delta T=.12\pm.01$°C; Figure 1C) was lower than that during the 3D MP-RAGE sequence (SAR=.064W/kg; $\Delta T=.27\pm.01$°C; Figure 1C). Neither GRE-EPI nor MP-RAGE sequence produced predicted SAR values in excess of the vendor-specified .1W/kg safety SAR threshold to prevent adverse effects during MRI of patients with an implanted DBS system.[38]

STN DBS evokes BOLD signal activation in motor and non-motor circuitry

To characterize the circuitry affected by STN DBS (2V 185Hz 90μs pulse width in 10 subjects, 2V 130Hz 90 μs) in patients with PD, 10 patients underwent intraoperative fMRI during DBS. BOLD signal activation was detected in several regions of the sensorimotor network, including ipsilateral primary motor and somatosensory cortices, bilateral premotor cortex, ipsilateral supplementary motor area (SMA), thalamus (dorsal medial nucleus), caudate, and peduncolopontine nucleus, and bilateral cerebellum (Figure 2A). Maximum t-scores were detected within ipsilateral premotor cortex/SMA (t=8.82) and primary motor cortex (t=8.75). Furthermore, activation was detected in limbic and associative areas, and in the bilateral precuneus and cuneus regions was observed (Figure 2A; Table 2).

To study the time course of DBS-evoked fMRI BOLD activation in each of three functionally-defined ROIs (SMA, premotor/primary motor and somatosensory association), an event-related averaging analysis was performed. The resulting time courses revealed peak BOLD signal percent change between .25–.40% in each of the ROIs within 5 frames (15 seconds) of stimulation onset (Figure 2B).

Cortex Based Alignment

A cortex-based alignment was performed to better resolve the overlapping cortical ROIs in the midline. This alignment revealed more distinct regions of activation in ipsilateral SMA, primary motor cortex, premotor cortex, primary somatosensory cortex, anterior cingulate cortex, thalamus, PPN and visual cortex. Contralateral posterior cingulate cortex, precuneus, and visual cortex showed activation (Figure 3).

Anesthesia vs. Awake State

To assess the effect of anesthesia on the patterns of DBS-induced fMRI activation, patients were sub-divided into those who were studied under anesthesia (n=5) versus those who were studied awake (n=5). Interestingly, as shown in Figure 4, the areas of activation were similar regardless of anesthesia state, but the signal strength was much stronger and in the awake state, significant at the FDR<.01 in the awake state as compared to the FDR<.05 level in the anesthesia state (Figure 4B).

Discussion

In this study, we aimed to implement intra-OR-fMRI for the investigation of DBS mechanisms in PD patients. To date, only a few groups have performed fMRI during STN DBS, due to the potential risks associated with MRI acquisition in patients with DBS implants, which include local tissue heating in the brain.[39]

MRI safety during DBS

There is large variability between measured RF-heating reported by different groups,[39–41] suggesting lack of generalizability of these findings and underscoring the importance of performing site-specific safety testing experiments.[36] The present study was conducted in accordance with the manufacturer's DBS-MRI safety guidelines.[42] We performed a phantom test reporting maximum temperature increases below the 1°C safety threshold for

this study, which is consistent with our previous large animal *in vivo* safety study report.[40] Average head SAR values of less than 0.02W/kg were recorded during the fMRI study in all the patients, and an MR physicist with expertise in MRI for patients with implanted electronic devices was present during all sessions.

fMRI for DBS

Previous STN DBS functional network studies strongly suggest that STN DBS exerts distributed effects throughout motor network structures, including premotor and motor cortices, thalamus, and contralateral cerebellum. However, reports of DBS-evoked modulation of non-motor networks have been somewhat variable, likely due to differences between studies in patient numbers and disease-state characteristics, as well as experimental methods.[43]

Jech et al. were the first to report the network effects of STN DBS using fMRI in three patients.[28] Stimulation-evoked BOLD signal increases were observed in ipsilateral motor areas including thalamus, globus pallidus, and premotor cortex. A similarly-designed experiment in a single subject corroborated these findings,[29] showing BOLD increases in motor regions (premotor, SMA, primary motor cortex, cerebellum, putamen, and thalamus), while also detecting changes in non-motor areas (mediodorsal thalamus, parietal lobe, bilateral parahippocampal gyri, posterior cingulate). In a series of five patients, STN DBS-evoked motor activation (ipsilateral basal ganglia and motor cortex, and contralateral cerebellum) with 3T fMRI, in line with previous studies.[32] The effect of DBS on non-motor, in addition to motor networks, corroborates the results of previous PET studies, which have reported DBS-evoked activations in primary motor cortex, SMA, premotor cortex, prefrontal cortex, cerebellum, thalamus, basal ganglia, and cingulate cortex.[44–49]

The effect of DBS on resting state fMRI networks has also been examining the effective connectivity in twelve PD patients.[17] Their findings support the role of STN stimulation in modulating the basal ganglia direct and indirect pathways, the hyperdirect pathway between the STN, the cortex, the cortico-striatal and thalamo-cortical pathways. Together, these studies suggest that the clinically effective stimulation was found to alter inter-regional coupling within the motor cortico-striato-thalamo-cortical loop, concordant with the current hypothesis of DBS functioning.[13–15,17,50,51]

Our findings, both in large animals[33,34] and in the present study, reports STN stimulation affects in both ipsilateral and contralateral motor cortices, a phenomenon previously reported in clinical,[52] and partially explainable by antidromic activation of STN bilateral afferents from the motor cortices. Stimulation-induced antidromic and orthodromic activation of regions functionally connected to the STN is legitimated also by results from other groups adopting neurophysiological and functional imaging techniques, supporting the hypothesis that modulation of the STN activity may lead to normalization of neural activity in areas such as the primary motor, premotor, and SMA, that are known to be hypo-functioning in PD patients.[16,46,53–56]

In our study, to further test the statistical significance of the observed motor network activation, we applied a more stringent Bonferroni correction (<0.001). The BOLD signal

increase was still significant mainly in the motor network including ipsilateral primary motor, premotor, SMA, PPN, cingulate gyrus, and in the contralateral cerebellum. However, we did not observe equally preserved non-motor network activation, indicating that the effect of STN DBS on these areas presents higher inter-subject variability. In addition, to minimize the effect that the inter-subject anatomical variability in gyri and sulci has on normalization in multi-subject analysis, we performed a cortex-based alignment. This approach confirmed segregated activation in the primary motor and premotor cortices, SMA, and primary somatosensory areas by STN DBS.

In addition to cortical activity, the PPN is one of the areas detected in both our human and large animal series.[33,34] The PPN is known to have an important role in motor functions and gait control, and to have reciprocal connections with the STN.[57] These elements suggest that the PPN may be an important mediator of DBS STN efficacy, and support the exploration of this site as a possible stimulation target for motor disorders.[58–60]

Our findings from ten patients are consistent not only with the ones from our animal studies, but also with results from previous human case reports and series, even though characterized by different experimental settings. Importantly, the ROIs detected in our series include all of those that were partially reported in the described previous studies. Functional circuitry effect of DBS might vary as a function of targeting accuracy, individual disease-state variance, and stimulation parameter programming.[61] Since most of the ROIs that we detected in our study have been sparsely described in previous reports, we believe that the larger population number increased the power of the analysis, bringing many ROIs to higher significance levels.

In addition to the prominent motor circuitry activation, activation of cognitive and emotional circuitry was observed, including ipsilateral dorsal anterior cingulate, orbitofrontal, and insula, and contralateral parahippocampus. This is consistent in patients with more ventral STN DBS,[29] as well as with the anatomical connectivity of ventromedial STN.[62] This activation may be of particular interest in light of several reports of adverse cognitive and emotional effects, reporting decrease verbal fluency, worsening of apathy and thought disorders, with reports of suicidality and hypomania.[62–67] Finally, insula shown to be affected by STN DBS, is being revisited as the central hub for processing relevant information related to the state of the body as well as cognitive and mood states in PD.[68]

Limitations

FMRI acquisition on the day of electrode implantation (n=5) may have been confounded by micro-lesion effects.[69] Additionally, as seen in Supplementary Figure 1, while the DBS electrode produced minimal artifact, the extension wire connector produced prominent susceptibility artifact. This might have created signal loss in the temporal lobe, ventral sensory cortices and parietal lobe. Finally, our study is limited to seeing short-term effect of DBS, as there are possible long-term synaptic plasticity effects reported.[70]

Conclusions

Functional neuroimaging, including fMRI and PET, has an important role in studying DBS mechanisms, due to its wide clinical availability and ability to assess global functional neural activity. While PET provides molecular specificity and safe application in the context of implanted electrical devices, its disadvantage is the limited flexibility in experimental designs, due to the radioisotope washout time and the consequent limit of testing limited number of DBS parameter per day. FMRI, on the other hand, allows experimenters to test differences among varying DBS stimulating contacts and stimulation parameters in a single relatively short session.

This study has demonstrated BOLD signal activation of both motor and non-motor circuitry, whereas the motor network activation showed more consistency throughout the subjects compared to non-motor network activity with STN DBS in PD using intra-OR-fMRI. This technique allows for a relatively quick scan time during which stimulation parameters can be dynamically manipulated, and therefore holds potential interest to provide insight into the therapeutic outcome and/or adverse effects of during DBS surgery. This may become increasingly important as DBS indications continually expand to include treatment of non-motor disorders, in which therapeutic outcome is more subjective and difficult to measure.

Supplementary Material

Refer to Web version on PubMed Central for supplementary material.

Acknowledgments

Financial support This work was supported in part by NIH (R01 NS 70872 award to KHL), CCaTS Career Transition Award to SYC and The Grainger Foundation. EJK was supported by the National Institute of General Medical Sciences (T32 GM 65841) and the National Center for Advancing Translational Science (NCATS; TL1 TR000137).

Abbreviations

DBS	deep brain stimulation
PD	Parkinson’s disease
STN	subthalamic nucleus
PPN	pedunculopontine nucleus
NHP	non-human primate
PET	positron emission tomography
fMRI	functional magnetic resonance imaging
GE-EPI	gradient echo-echo planar imaging
RF	radio frequency
SAR	specific absorption rate
FWHM	full width at half maximum

SMA supplementary motor area

References

1. Benabid AL, Chabardes S, Mitrofanis J, Pollak P. Deep brain stimulation of the subthalamic nucleus for the treatment of Parkinson's disease. The Lancet. Neurology. Jan; 2009 8(1):67–81. [PubMed: 19081516]
2. Starr PA, Vitek JL, Bakay RA. Deep brain stimulation for movement disorders. Neurosurgery clinics of North America. Apr; 1998 9(2):381–402. [PubMed: 9495900]
3. Pereira EA, Green AL, Stacey RJ, Aziz TZ. Refractory epilepsy and deep brain stimulation. Journal of clinical neuroscience: official journal of the Neurosurgical Society of Australasia. Jan; 2012 19(1):27–33. [PubMed: 22172283]
4. Moore NZ, Lempka SF, Machado A. Central neuromodulation for refractory pain. Neurosurgery clinics of North America. Jan; 2014 25(1):77–83. [PubMed: 24262901]
5. Greenberg BD, Rauch SL, Haber SN. Invasive circuitry-based neurotherapeutics: stereotactic ablation and deep brain stimulation for OCD. Neuropsychopharmacology: official publication of the American College of Neuropsychopharmacology. Jan; 2010 35(1):317–336. [PubMed: 19759530]
6. Visser-Vandewalle V, Temel Y, Boon P, et al. Chronic bilateral thalamic stimulation: a new therapeutic approach in intractable Tourette syndrome. Report of three cases. Journal of neurosurgery. Dec; 2003 99(6):1094–1100. [PubMed: 14705742]
7. Lozano AM, Giacobbe P, Hamani C, et al. A multicenter pilot study of subcallosal cingulate area deep brain stimulation for treatment-resistant depression. Journal of neurosurgery. Feb; 2012 116(2):315–322. [PubMed: 22098195]
8. Odekerken VJJ, van Laar T, Staal MJ, et al. Subthalamic nucleus versus globus pallidus bilateral deep brain stimulation for advanced Parkinson's disease (NSTAPS study): a randomised controlled trial. The Lancet Neurology. 2013; 12(1):37–44. [PubMed: 23168021]
9. Funkiewiez A, Ardouin C, Krack P, et al. Acute psychotropic effects of bilateral subthalamic nucleus stimulation and levodopa in Parkinson's disease. Movement disorders: official journal of the Movement Disorder Society. May; 2003 18(5):524–530. [PubMed: 12722166]
10. Hamani C, Saint-Cyr JA, Fraser J, Kaplitt M, Lozano AM. The subthalamic nucleus in the context of movement disorders. Brain: a journal of neurology. Jan; 2004 127(Pt 1):4–20. [PubMed: 14607789]
11. Mallet L, Schupbach M, N'Diaye K, et al. Stimulation of subterritories of the subthalamic nucleus reveals its role in the integration of the emotional and motor aspects of behavior. Proceedings of the National Academy of Sciences of the United States of America. Jun 19; 2007 104(25):10661–10666. [PubMed: 17556546]
12. Krack P, Hariz MI, Baunez C, Guridi J, Obeso JA. Deep brain stimulation: from neurology to psychiatry? Trends in neurosciences. Oct; 2010 33(10):474–484. [PubMed: 20832128]
13. DeLong M, Wichmann T. Deep brain stimulation for movement and other neurologic disorders. Annals of the New York Academy of Sciences. Aug.2012 1265:1–8. [PubMed: 22823512]
14. McIntyre CC, Grill WM, Sherman DL, Thakor NV. Cellular effects of deep brain stimulation: model-based analysis of activation and inhibition. Journal of neurophysiology. Apr; 2004 91(4):1457–1469. [PubMed: 14668299]
15. Asanuma K, Tang C, Ma Y, et al. Network modulation in the treatment of Parkinson's disease. Brain: a journal of neurology. Oct; 2006 129(Pt 10):2667–2678. [PubMed: 16844713]
16. Li Q, Ke Y, Chan DC, et al. Therapeutic deep brain stimulation in Parkinsonian rats directly influences motor cortex. Neuron. Dec 6; 2012 76(5):1030–1041. [PubMed: 23217750]
17. Kahan J, Urner M, Moran R, et al. Resting state functional MRI in Parkinson's disease: the impact of deep brain stimulation on 'effective' connectivity. Brain: a journal of neurology. Apr; 2014 137(Pt 4):1130–1144. [PubMed: 24566670]

18. Cunic D, Roshan L, Khan FI, Lozano AM, Lang AE, Chen R. Effects of subthalamic nucleus stimulation on motor cortex excitability in Parkinson's disease. Neurology. 2002; 58(11):1665–1672. [PubMed: 12058096]
19. Dauper J, Peschel T, Schrader C, et al. Effects of subthalamic nucleus (STN) stimulation on motor cortex excitability. Neurology. 2002; 59(5):700–706. [PubMed: 12221160]
20. Fraix V, Pollak P, Vercueil L, Benabid AL, Mauguiere F. Effects of subthalamic nucleus stimulation on motor cortex excitability in Parkinson's disease. Clinical neurophysiology: official journal of the International Federation of Clinical Neurophysiology. Nov; 2008 119(11):2513–2518. [PubMed: 18783985]
21. Dejean C, Hyland B, Arbuthnott G. Cortical effects of subthalamic stimulation correlate with behavioral recovery from dopamine antagonist induced akinesia. Cerebral cortex. May; 2009 19(5):1055–1063. [PubMed: 18787234]
22. Kuriakose R, Saha U, Castillo G, et al. The nature and time course of cortical activation following subthalamic stimulation in Parkinson's disease. Cerebral cortex. Aug; 2010 20(8):1926–1936. [PubMed: 20019146]
23. Devergnas A, Wichmann T. Cortical potentials evoked by deep brain stimulation in the subthalamic area. Frontiers in systems neuroscience. 2011; 5:30. [PubMed: 21625611]
24. Brunenberg EJ, Moeskops P, Backes WH, et al. Structural and resting state functional connectivity of the subthalamic nucleus: identification of motor STN parts and the hyperdirect pathway. PloS one. 2012; 7(6):e39061. [PubMed: 22768059]
25. Gradinaru V, Mogri M, Thompson KR, Henderson JM, Deisseroth K. Optical deconstruction of parkinsonian neural circuitry. Science. Apr 17; 2009 324(5925):354–359. [PubMed: 19299587]
26. Obeso I, Ray NJ, Antonelli F, Cho SS, Strafella AP. Combining functional imaging with brain stimulation in Parkinson's disease. International review of psychiatry. Oct; 2011 23(5):467–475. [PubMed: 22200136]
27. Ceballos-Baumann AO, Boecker H, Bartenstein P, et al. A positron emission tomographic study of subthalamic nucleus stimulation in Parkinson disease: enhanced movement-related activity of motor-association cortex and decreased motor cortex resting activity. Archives of neurology. Aug; 1999 56(8):997–1003. [PubMed: 10448806]
28. Jech R, Urgosik D, Tintera J, et al. Functional magnetic resonance imaging during deep brain stimulation: a pilot study in four patients with Parkinson's disease. Movement disorders: official journal of the Movement Disorder Society. Nov; 2001 16(6):1126–1132. [PubMed: 11748747]
29. Stefurak T, Mikulis D, Mayberg H, et al. Deep brain stimulation for Parkinson's disease dissociates mood and motor circuits: a functional MRI case study. Movement disorders: official journal of the Movement Disorder Society. Dec; 2003 18(12):1508–1516. [PubMed: 14673888]
30. Hesselmann V, Sorger B, Girnus R, et al. Intraoperative functional MRI as a new approach to monitor deep brain stimulation in Parkinson's disease. European radiology. Apr; 2004 14(4):686–690. [PubMed: 14513267]
31. Arantes PR, Cardoso EF, Barreiros MA, et al. Performing functional magnetic resonance imaging in patients with Parkinson's disease treated with deep brain stimulation. Movement disorders: official journal of the Movement Disorder Society. Aug; 2006 21(8):1154–1162. [PubMed: 16671094]
32. Phillips MD, Baker KB, Lowe MJ, et al. Parkinson disease: pattern of functional MR imaging activation during deep brain stimulation of subthalamic nucleus--initial experience. Radiology. Apr; 2006 239(1):209–216. [PubMed: 16567487]
33. Min HK, Hwang SC, Marsh MP, et al. Deep brain stimulation induces BOLD activation in motor and non-motor networks: an fMRI comparison study of STN and EN/GPi DBS in large animals. NeuroImage. Nov 15; 2012 63(3):1408–1420. [PubMed: 22967832]
34. Min HK, Ross EK, Lee KH, et al. Subthalamic nucleus deep brain stimulation induces motor network BOLD activation: use of a high precision MRI guided stereotactic system for nonhuman primates. Brain stimulation. Jul-Aug;2014 7(4):603–607. [PubMed: 24933029]
35. Standard Test Method for Measurement of Radio Frequency Induced Heating On or Near Passive Implants During Magnetic Resonance Imaging. American Society for Testing and Materials (ASTM) International; West Conshohocken, PA: 2011. F2182-11a A.

36. Baker KB, Tkach JA, Nyenhuis JA, et al. Evaluation of specific absorption rate as a dosimeter of MRI-related implant heating. Journal of magnetic resonance imaging: JMRI. Aug; 2004 20(2): 315–320. [PubMed: 15269959]
37. Bland JM, Altman DG. Multiple significance tests: the Bonferroni method. Bmj. Jan 21.1995 310(6973):170. [PubMed: 7833759]
38. Medtronic. MRI guidelines for medtronic deep brain stimulation systems. 2010
39. Carmichael DW, Pinto S, Limousin-Dowsey P, et al. Functional MRI with active, fully implanted, deep brain stimulation systems: safety and experimental confounds. NeuroImage. Aug 15; 2007 37(2):508–517. [PubMed: 17590355]
40. Gorny KR, Presti MF, Goerss SJ, et al. Measurements of RF heating during 3.0-T MRI of a pig implanted with deep brain stimulator. Magnetic resonance imaging. Jun; 2013 31(5):783–788. [PubMed: 23228310]
41. Spiegel J, Fuss G, Backens M, et al. Transient dystonia following magnetic resonance imaging in a patient with deep brain stimulation electrodes for the treatment of Parkinson disease. Case report. Journal of neurosurgery. Oct; 2003 99(4):772–774. [PubMed: 14567615]
42. Larson PS, Richardson RM, Starr PA, Martin AJ. Magnetic resonance imaging of implanted deep brain stimulators: experience in a large series. Stereotactic and functional neurosurgery. 2008; 86(2):92–100. [PubMed: 18073522]
43. Boertien T, Zrinzo L, Kahan J, et al. Functional imaging of subthalamic nucleus deep brain stimulation in Parkinson's disease. Movement disorders: official journal of the Movement Disorder Society. Aug 15; 2011 26(10):1835–1843. [PubMed: 21674623]
44. Strafella AP, Dagher A, Sadikot AF. Cerebral blood flow changes induced by subthalamic stimulation in Parkinson's disease. Neurology. 2003; 60(6):1039–1042. [PubMed: 12654980]
45. Sestini S, Ramat S, Formiconi AR, Ammannati F, Sorbi S, Pupi A. Brain networks underlying the clinical effects of long-term subthalamic stimulation for Parkinson's disease: a 4-year follow-up study with rCBF SPECT. Journal of nuclear medicine: official publication, Society of Nuclear Medicine. Sep; 2005 46(9):1444–1454.
46. Grafton ST, Turner RS, Desmurget M, et al. Normalizing motor-related brain activity: subthalamic nucleus stimulation in Parkinson disease. Neurology. Apr 25; 2006 66(8):1192–1199. [PubMed: 16636237]
47. Karimi M, Golchin N, Tabbal SD, et al. Subthalamic nucleus stimulation-induced regional blood flow responses correlate with improvement of motor signs in Parkinson disease. Brain: a journal of neurology. Oct; 2008 131(Pt 10):2710–2719. [PubMed: 18697909]
48. Kalbe E, Voges J, Weber T, et al. Frontal FDG-PET activity correlates with cognitive outcome after STN-DBS in Parkinson disease. Neurology. Jan 6; 2009 72(1):42–49. [PubMed: 19122029]
49. Hill KK, Campbell MC, McNeely ME, et al. Cerebral blood flow responses to dorsal and ventral STN DBS correlate with gait and balance responses in Parkinson's disease. Experimental neurology. Mar.2013 241:105–112. [PubMed: 23262122]
50. Liu Y, Postupna N, Falkenberg J, Anderson ME. High frequency deep brain stimulation: what are the therapeutic mechanisms? Neuroscience and biobehavioral reviews. 2008; 32(3):343–351. [PubMed: 17187859]
51. Kahan J, Mancini L, Urner M, et al. Therapeutic subthalamic nucleus deep brain stimulation reverses cortico-thalamic coupling during voluntary movements in Parkinson's disease. PloS one. 2012; 7(12):e50270. [PubMed: 23300524]
52. Kumar R, Lozano AM, Sime E, Halket E, Lang AE. Comparative effects of unilateral and bilateral subthalamic nucleus deep brain stimulation. Neurology. Aug 11; 1999 53(3):561–566. [PubMed: 10449121]
53. Fraix V, Pollak P, Vercueil L, Benabid AL, Mauguiere F. Effects of subthalamic nucleus stimulation on motor cortex excitability in Parkinson's disease. Clinical neurophysiology: official journal of the International Federation of Clinical Neurophysiology. Nov; 2008 119(11):2513–2518. [PubMed: 18783985]
54. Devergnas A, Wichmann T. Cortical potentials evoked by deep brain stimulation in the subthalamic area. Frontiers in systems neuroscience. 2011; 5:30. [PubMed: 21625611]

55. DeLong M, Wichmann T. Deep brain stimulation for movement and other neurologic disorders. Annals of the New York Academy of Sciences. Aug.2012 1265:1–8. [PubMed: 22823512]
56. Paschali A, Constantoyannis C, Angelatou F, Vassilakos P. Perfusion brain SPECT in assessing motor improvement after deep brain stimulation in Parkinson's disease. Acta neurochirurgica. Mar; 2013 155(3):497–505. [PubMed: 23334750]
57. Neagu B, Tsang E, Mazzella F, et al. Pedunculopontine nucleus evoked potentials from subthalamic nucleus stimulation in Parkinson's disease. Experimental neurology. Dec.2013 250:221–227. [PubMed: 24095981]
58. Lozano AM, Snyder BJ. Deep brain stimulation for parkinsonian gait disorders. Journal of neurology. Aug; 2008 255(Suppl 4):30–31. [PubMed: 18821083]
59. Strafella AP, Lozano AM, Ballanger B, Poon YY, Lang AE, Moro E. rCBF changes associated with PPN stimulation in a patient with Parkinson's disease: a PET study. Movement disorders: official journal of the Movement Disorder Society. May 15; 2008 23(7):1051–1054. [PubMed: 18412282]
60. Ballanger B, Lozano AM, Moro E, et al. Cerebral blood flow changes induced by pedunculopontine nucleus stimulation in patients with advanced Parkinson's disease: a [(15)O] H2O PET study. Human brain mapping. Dec; 2009 30(12):3901–3909. [PubMed: 19479730]
61. Okun MS, Foote KD. Parkinson's disease DBS: what, when, who and why? The time has come to tailor DBS targets. Expert review of neurotherapeutics. Dec; 2010 10(12):1847–1857. [PubMed: 21384698]
62. Volkmann J, Daniels C, Witt K. Neuropsychiatric effects of subthalamic neurostimulation in Parkinson disease. Nature reviews. Neurology. Sep; 2010 6(9):487–498.
63. Campbell MC, Karimi M, Weaver PM, et al. Neural correlates of STN DBS-induced cognitive variability in Parkinson disease. Neuropsychologia. Nov; 2008 46(13):3162–3169. [PubMed: 18682259]
64. Cilia R, Siri C, Marotta G, et al. Brain networks underlining verbal fluency decline during STN-DBS in Parkinson's disease: an ECD-SPECT study. Parkinsonism & related disorders. Jul; 2007 13(5):290–294. [PubMed: 17292655]
65. Jahanshahi M, Ardouin CM, Brown RG, et al. The impact of deep brain stimulation on executive function in Parkinson's disease. Brain: a journal of neurology. Jun; 2000 123(Pt 6):1142–1154. [PubMed: 10825353]
66. Schroeder U, Kuehler A, Haslinger B, et al. Subthalamic nucleus stimulation affects striato-anterior cingulate cortex circuit in a response conflict task: a PET study. Brain: a journal of neurology. Sep; 2002 125(Pt 9):1995–2004. [PubMed: 12183345]
67. Thobois S, Hotton GR, Pinto S, et al. STN stimulation alters pallidal-frontal coupling during response selection under competition. Journal of cerebral blood flow and metabolism: official journal of the International Society of Cerebral Blood Flow and Metabolism. Jun; 2007 27(6): 1173–1184.
68. Christopher L, Koshimori Y, Lang AE, Criaud M, Strafella AP. Uncovering the role of the insula in non-motor symptoms of Parkinson's disease. Brain: a journal of neurology. Aug; 2014 137(Pt 8):2143–2154. [PubMed: 24736308]
69. Tasker RR. Deep brain stimulation is preferable to thalamotomy for tremor suppression. Surgical neurology. Feb; 1998 49(2):145–153. discussion 153–144. [PubMed: 9457264]
70. van Hartevelt TJ, Cabral J, Deco G, et al. Neural plasticity in human brain connectivity: the effects of long term deep brain stimulation of the subthalamic nucleus in Parkinson's disease. PloS one. 2014; 9(1):e86496. [PubMed: 24466120]

A.

B.

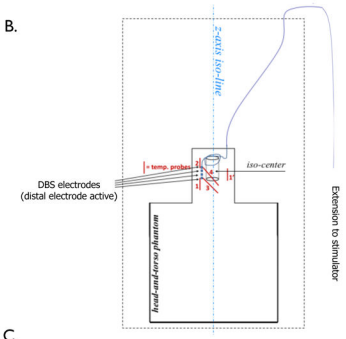

C.

Pulse Sequence	SAR (W/kg)	ΔTmax (°C)
GE-EPI (fMRI)	.016	.12±0.01
3D MP-RAGE	.064	.27±0.01

Figure 1. Intraoperative fMRI setup and Phantom Testing

A) Photograph of the intraoperative MRI suite. B) Schematic drawing of the anthropomorphic phantom in the MR bore illustrating placement extension wiring (purple), positioning of DBS electrode, and placement of temperature probes (red) on the proximal and distal DBS electrode contacts. C) Plot of change in temperature (°C) vs. time (sec) during a series of pulse sequences: A- MP-RAGE, stimulation on, wires along iso-line (SAR=.064W/kg; ΔT_{max}=.27±.01°C) C-GE-EPI, stimulation on, wires along iso-line (SAR=.016W/kg; ΔT_{max}=.12±.01°C); Temperature data shown were sampled at 1sec intervals smoothed using a 20-point running average.

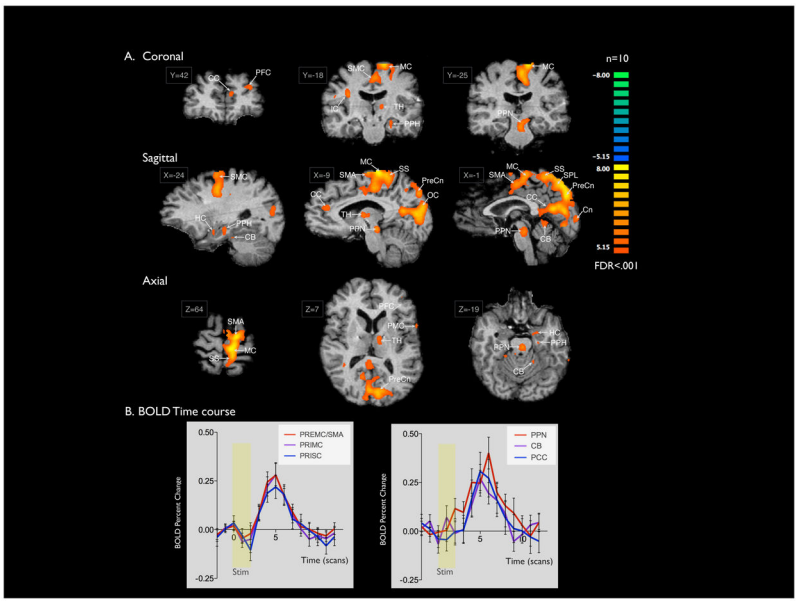

Figure 2. BOLD signal activation with STN DBS (2V 130–185Hz 90μs) for PD

A) Areas of activation with unilateral STN stimulation at 2V 130–185Hz 90μs (n = 10) for PD. Slice Locations are presented in Talairach coordinates. Significant activation (FDR<. 001) was observed in bilateral premotor and primary motor cortices, precuneus, occipital lobes, cerebellum, and anterior and posterior cingulate. Activation of ipsilateral thalamus, pedunculopontine nucleus, parahippocampal gyrus, and hippocampus, and contralateral insula were also observed. B) The average time courses for five regions of interest were plotted as average percent change in BOLD signal from baseline vs. time (one scan is equal to TR = 3 seconds) using ten frames (30 seconds) prior to stimulation (yellow box) as the baseline.

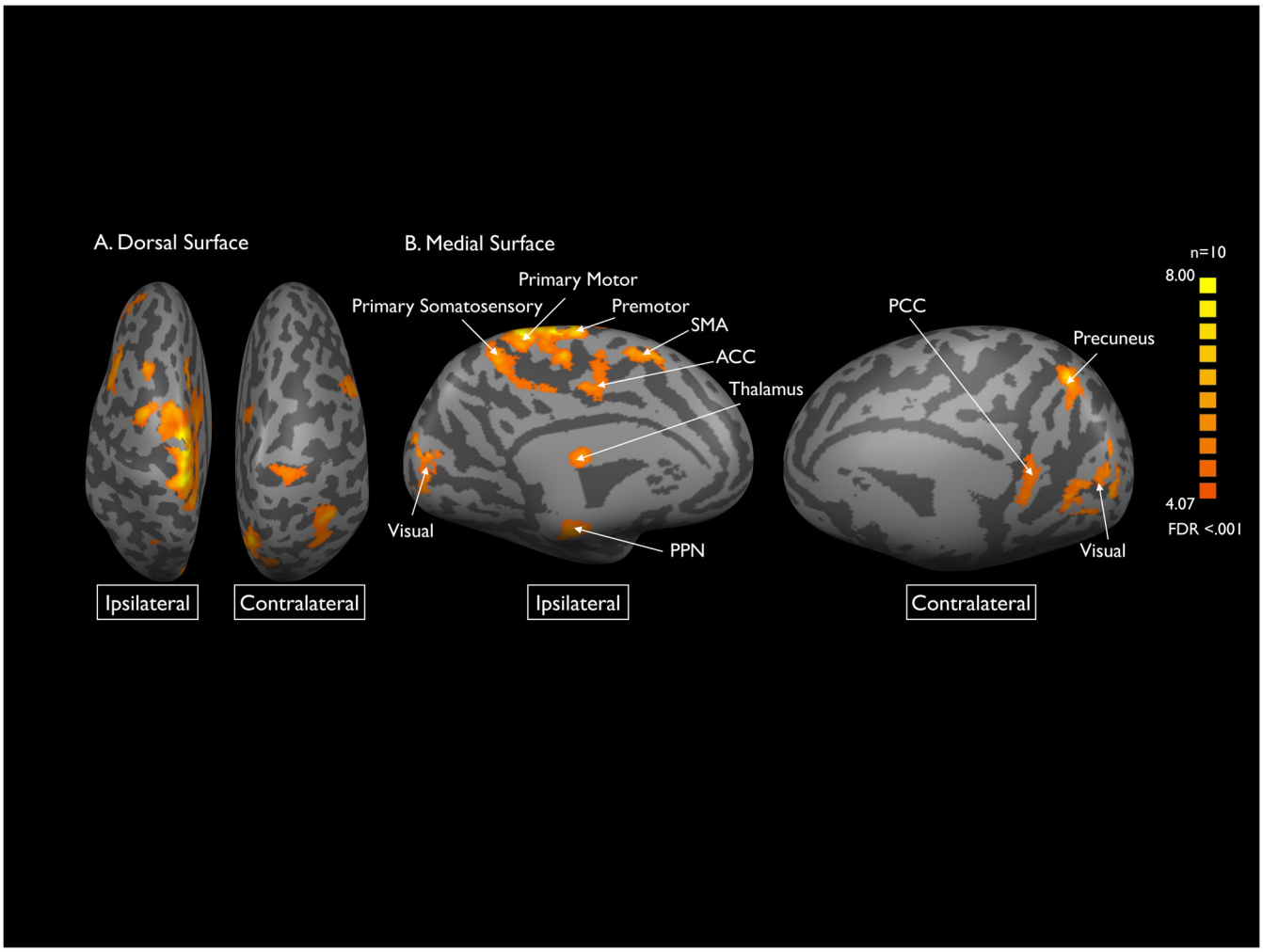

Figure 3. Sensorimotor BOLD signal activation with cortex-based alignment

Cortical areas of significant BOLD activation resolved by cortex based analysis projected on inflated representations of the dorsal (A) and medial (B) surfaces of the brain. Areas of activation included: bilateral supplementary motor and occipital lobes; ipsilateral primary motor, and primary and secondary somatosensory cortices, thalamus, anterior cingulate gyrus, and pedunculopontine nucleus, and contralateral precuneus (FDR <.001).

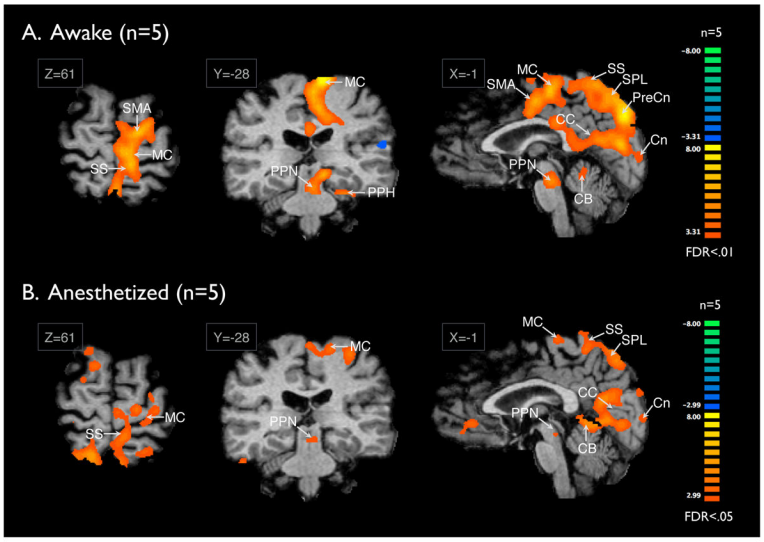

Figure 4. Awake vs Anesthetized

Comparison of BOLD activation during DBS conducted in the anesthetized (n=5) vs. awake state (n=5). The signal strength was much stronger and in the awake state, significant at the FDR<.01 as compared to FDR<.05 level in the anesthetized state.

Table 1

Clinical patient information.

Patient (Age, Gender)	Disease Duration (Years)	Preoperative UPDRS-III score (Off)	Preoperative I UPDRS-III score (On)	Postoperative UPDRS-III score (Off)	Follow-up UPDRS-III score (Off)	Follow-up (months)	Change in score at last follow-up (percent change)	Optimal contacts at follow-up	Optimal settings at follow-up	Stimulation side during fMRI
Patient 1 (60Y, M)	8	41	27	40	24	6	**41%**	Left 1-C+ Right 9-C+	Left 3.15V 60us 130 Hz Right 1.90V 60us 130 Hz	Left
Patient 2 (70Y, F)	11	21	7	21	8	2	**62%**	Left 0-C+	Left 1.65V 60us 130Hz	Left
Patient 3 (46Y, M)	14	37	2	26	8	13	**78%**	Left 2-C+ Right 10-C+	Left 2.90V 60us 130Hz Right 2.90V 60us 130Hz	Left
Patient 4 (62Y, M)	10	32	18	21	16	16	**50%**	Left 2-C+ Right 9-10+	Left 3.40V 60us 130Hz Right 2.40V 60us 130Hz	Left
Patient 5 (78Y, F)	1	27	26	19	21	5	**22%**	Left 0+1-2-3+ Right 8+9-10-11+	Left 2.50V 60us 130Hz Right 2.40V 60us 130Hz	Left
Patient 6 (61Y, M)	12	21	5	26	19	11	**10%**	Left 3-C+ Right 11-C+	Left 3.70V 60us 130Hz	Left

Patient (Age, Gender)	Disease Duration (Years)	Preoperative UPDRS-III score (Off)	Preoperative I UPDRS-III score (On)	Postoperative UPDRS-III score (Off)	Follow-up UPDRS-III score (Off)	Follow-up (months)	Change in score at last follow-up (percent change)	Optimal contacts at follow-up	Optimal settings at follow-up	Stimulation side during fMRI
									Right 3.75V 60us 130Hz Right 3.75V 60us 130Hz Right 3.75V 60us 130Hz Right 3.75V 60us 130Hz	
Patient 8 (54Y, F)	14	26	3	33	51	1	**−96%**	Left 3-C+ Right 11-10+	Left 2.00V 90us 130Hz Right 2.10V 90us 130Hz	Right
Patient 9 (57Y, F)	12	31	2	31	26	3	**16%**	Left 3-C+ Right 11-C+	Left 2.20V 90us 130Hz Right 2.20V 90us 130Hz	Right
Patient 10 (60Y, F)	16	35	16	34	28	2	**20%**	Left 3-C+ Right 11-C+	Left 2.40V 60us 130Hz Right 2.40V 60us 130Hz	Right
Total (N=9) mean [±SD]	11±4	30±7	12±10	28±7	22±13	7±5	**22±50%**			

Abbreviations: SD, standard deviation; UPDRS, Unified Parkinson's Disease Rating Scale.

Table 2

Areas of significant brain activation: regions of interest and corresponding Brodmann area, function, t-score and Talairach coordinates of the voxel with the peak t-score, size. Areas with increased BOLD-signal after Bonferroni correction (p<.001) are highlighted.

Anatomical Location	Functional Location	BA	Talairach Coordinates (x, y, z)	Size (mm^3)	Max t-Score
Premotor cortex, Supplementary motor area (I)	Motor	6	−11, −27, 68	10138	**8.82***
Primary motor cortex (I)	Motor	4	−10, −27, 68	5991	**8.75***
Precuneus (I)	Somatosensory association	7	2, −83, 33	5464	**8.25***
Occipital (C)	Visual	18,19	3, −83, 33	7986	**8.21***
Posterior cingulate (I)	Limbic	30	−4, −64, 14	3506	**8.02***
Precuneus (C)	Somatosensory association	7	3, −67, 51	3679	**7.76***
Occipital (I)	Visual	17,19	−14, −81, 12	10164	**7.65***
Primary Somatosensory cortex (I)	Somatosensory	3	−11, −40, 63	4859	**7.40***
Cingulate gyrus (I)	Limbic		−4, −25, 52	3850	**6.79***
Premotor cortex (C)	Motor	6	34, 6, 46	2274	**6.67***
Cerebellum (C)	Motor		3, −52, −5	903	**6.46***
Pedunculopontine nucleus (I)	Motor		−11, −28, −9	1617	**6.11***
Parahippocampal gyrus (I)	Limbic	28,35,36	−16, −12, −25	888	6.07
Caudate (I)	Motor		−25, −12, 35	121	5.79
Supramarginal gyrus (C)	Visuospatial	40	35, −47, 38	1383	5.77
Insula (C)	Limbic	13	33, −18, 26	399	5.39
Thalamus (I)	Motor		−10, −10, 9	528	5.34
Inferior frontal gyrus (I)	Language	45,47	−56, 8, −1	990	5.25
Superior parietal lobule (I)	Somatosensory association	7	−32, −60, 53	349	5.24
Posterior cingulate (C)	Limbic	29	3, −51, 12	709	5.23
Middle frontal gyrus (I)	Executive	10	−34, 37, 16	1021	5.03
Superior parietal lobule (C)	Somatosensory association	7	21, −59, 40	640	5.03
Cerebellum (I)	Motor		−21, −32, −23	80	4.90
Anterior cingulate (I)	Limbic	32	−8, 37, 19	355	4.89
Parahippocampal gyrus (C)	Limbic	36	24, −44, −17/41, −36, −6	80/40	4.87/−4.50

Anatomical Location	Functional Location	BA	Talairach Coordinates (x, y, z)	Size (mm^3)	Max t-Score
Inferior temporal gyrus (I)	Language, Visual	20,37	−64, −42, −23	574	4.86
Angular gyrus (I)	Language	39	−31, −64, 23	145	4.57
Middle temporal gyrus (I)	Auditory, Language	21	−45, −5, −16	73	4.55
Cingulate gyrus (C)	Limbic	31	12, −41, 34	111	4.54
Pons (C)			6, −34, −21	24	4.50
Postcentral gyrus (C)	Language,	3,43	51, −17, 22	53	4.44
Angular gyrus (C)	Visuospatial	39	36, −45, 7	42	4.40
Primary motor cortex (C)	Motor	4	17, −23, 50	25	4.26
Middle temporal gyrus (C)	Auditory	22	49, −44, −1	25	4.22
Supramarginal gyrus (I)	Language	40	−36, −54, 28/−56, −44, 20	29/110	4.20/−5.22
Orbitofrontal (C)	Associative	11	22, 41, −15	5	4.20
Inferior frontal gyrus (C)	Language	44	50, 0, 12	13	4.18
Superior temporal gyrus (C)	Cognition, Limbic	38	48, 13, −2	4	4.10
Dorsolateral prefrontal cortex (I)	Executive	46	−40, 45, 8	4	4.09
Fusiform gyrus(C)	Visual	37	34, −58, −5	8	4.08
Superior temporal gyrus (I)	Language	22	−43, −37, −1	46	−4.53

Abbreviations: BA: Brodmann Area; C: Contralateral; I: Ipsilateral

* Areas showing with Bonferroni correction P < .001